



Analytical solutions for elastic response of coated mesoporous materials to pore pressure



Mingchao Liu^a, Yafei Zhang^a, Jian Wu^a, Yixiang Gan^b, C.Q. Chen^{a,*}

^aDepartment of Engineering Mechanics, CNMM & AML, Tsinghua University, Beijing 100084, China

^bSchool of Civil Engineering, The University of Sydney, Sydney, NSW 2006, Australia

ARTICLE INFO

Article history:

Received 15 June 2016

Accepted 13 July 2016

Keywords:

Adsorption-induced deformation

Mesoporous material

Uniform and gradient coating

Pore-load modulus

ABSTRACT

Pore fluid adsorption-induced deformation of mesoporous materials is an important physical phenomenon. Experimental results show that the adsorption-induced elastic deformation can be quantified in terms of pore-load modulus (i.e., the ratio between pore pressure and overall strain). In practical applications, most mesoporous materials are functionalized by post-fabrication processes such as surface coating. In this paper, we develop a theoretical model to predict the adsorption-induced deformation of ordered mesoporous materials with uniform and functionally graded coatings. Closed-form solutions of the pore-load modulus are obtained as a function of porosity, elastic properties of bulk materials and coating phases, thickness of coating, and geometrical arrangement of pores. Deformation of a coated triangular lattice of cylindrical pores representing the mesoporous materials with inner fluid pressure is also simulated by the finite element method, showing excellent agreement with the established theoretical solutions. The proposed model provides a general description of the elastic response of heterogeneous mesoporous materials subjected to the inner pressure loading.

© 2016 Elsevier Ltd. All rights reserved.

1. Introduction

Mesoporous materials with ordered porous networks have attracted increasing attention in recent years, due to their broad range of applications including optoelectronics, sensors, and separation technologies (Amato, Delerue, & Von-Bardeleben, 1998; Canham, 2014; Davis, 2002; Sailor, 2012). Understanding of the relationship between their mechanical properties and pore structures is necessary to fulfill their functional applications (Canham, 2014; Sailor, 2012). Most previous works focus on the effective properties of the porous samples, such as the bulk and Young's moduli (e.g., Bellet, Lamagnere, Vincent, & Brechet, 1996; David & Zimmerman, 2011; Dourdain, Britton, Reichert, & Gibaud, 2008; Niu & Yan, 2015), to characterize the elastic response to external mechanical loads. For the applications of gas or fluid adsorption in mesoporous materials, the porous solids may contract or expand due to the physical and/or chemical interactions between the guest molecules and the solid pore walls (Gor & Neimark, 2010, 2011; Rasaiah, Garde, & Hummer, 2008). This phenomenon is called as the adsorption-induced deformation and is common in various porous media with ordered channel-like pores (Dolino, Bellet, & Faivre, 1996; Herman, Day, & Beamish, 2006; Kucheyev, Bradby, Williams, Jagadish, & Swain, 2002). Recently, the issue of adsorption-induced deformation has received renewed attention due to their potential applications of sensors and actuators in engineering applications (Biener et al., 2009; Melde, Johnson, & Charles, 2008).

* Corresponding author.

E-mail address: chencq@tsinghua.edu.cn (C.Q. Chen).

Owing to the recent advances in reliable experimental techniques, such as in situ small-angle X-ray and neutron diffractometry (Muroyama et al., 2008), one can easily measure the adsorption deformation for highly ordered mesoporous materials (Findenegg, Jähnert, Mütter, Prass, & Paris, 2010; Grosman, Puibasset, & Rolley, 2015; Prass, Mütter, Fratzl, & Paris, 2009). The measured adsorption-induced strain is a function of capillary pressure which acts as a radial stress on the pore walls and can be basically described by the Kelvin–Laplace equation (Horikawa, Do, & Nicholson, 2011). The ratio between the pore pressure and the overall deformation of the porous sample is defined as an effective elastic constant called as the pore-load modulus (Prass et al., 2009). Experimental results show that pore-load modulus can be expressed as a function of porosity and is also related to the elastic constants of the matrices. In order to quantitatively describe the aforementioned relationship, there are several theoretical models proposed in recent years (Dolino et al., 1996; Findenegg et al., 2010; Gor et al., 2015; Grosman et al., 2015; Günther, Prass, Paris, & Schoen, 2008; Liu, Wu, Gan, & Chen, 2016; Prass et al., 2009). One of the representative analytical model is given by Gor et al. (2015), where a single cylinder pore is taken as the unit cell. By adopting the elastic solution of a pressurized thick-walled cylinder, the engineering strain of the single unit cell is calculated and assumed to be equal to the overall elastic strain. On this basis, Liu et al. (2016) proposed a size-dependent theoretical model for the pore-load modulus to take into account the influence of surface energy. It has been shown that the size effect is significant when the pore size reduces to nano-scale. However, the surface effect is negligible when the pore size is larger than several tens of nanometers.

The main advantages of fabricating mesoporous materials include the flexibility of the synthesis routes and the possibility of using different types of post-fabrication processes (Innocenzi & Malfatti, 2013). Thus, one can design and produce a desired material with a particular functionality and microstructure. In practical applications, in order to improve surface stability for catalytic reactions and control the pore size and topography of the pore wall, most of the mesoporous materials are functionalized by surface treatment after the synthesis processes (El Kadib, Finiels, & Brunel, 2013; Feng et al., 1997; McInnes et al., 2015; Van Rhijn, De Vos, Sels, & Bossaert, 1998). Mesoporous materials have also been integrated in different ways in functional coatings for self-cleaning, hydrophobic, and antireflective applications (Fateh, Ismail, Dillert, & Bahnemann, 2011; Faustini et al., 2010). It should be noted that the coating layer of the mesoporous materials affect their overall physical properties, particularly the mechanical properties (Chen et al., 2015; Duan, Wang, Karihaloo, & Huang, 2006; Wang & Pindera, 2016). However, there are less theoretical models to describe the influence of surface coating on the adsorption-induced deformation of mesoporous materials.

In this paper, the contribution of surface coating is taken into account for the elastic response of ordered mesoporous materials subjected to inner pressure. By extending the micromechanical model of homogeneous ordered porous materials to the coated mesoporous materials, a theoretical framework with coating effect on the pore-load modulus of ordered mesoporous materials is developed. Note that the pore size of the considered mesoporous materials are assumed to larger than tens of nanometers. Under such a condition, the surface effect is negligible (Liu et al., 2016). Two typical coating structures are considered, i.e., uniform coating and functionally graded coating. Both can be generated by corresponding surface coating technologies (Birman, 2014; Bonfoh, Coulibaly, & Sabar, 2014; Cherkaoui, Sabar, & Berveiller, 1995; Mohammadi, Saha, & Akbarzadeh, 2016; Sburlati, 2012). In order to validate the proposed analytical models, the pore-load modulus of cylindrical pores distributed on a triangular lattice is calculated numerically using the finite element method (FEM) for both the uniform and gradient coating. The analytical predictions are in good agreement with the FEM results.

2. Theoretical analysis of the pore-load modulus

Consider a typical ordered mesoporous material shown in Fig. 1(a). The cylindrical pores are arranged on a well ordered as two-dimensional (2D) triangular lattice. Gor et al. (2015) pointed out that the overall dilatational strain in the plate with many pores can be approximated by the engineering strain of the unit cell of a homogeneous pressurized cylinder with free outer surface. Liu et al. (2016) further showed that each unit cell is affected by its neighboring cylinders, implying that the outer boundary conditions of the cylinder are related to the geometrical arrangement of the pores. Considering the thickness of the plate is much larger than the pore diameter, the porous plate can be regards as under plane strain condition. Ignoring the surface effect, the pore-load modulus can be obtained as (Liu et al., 2016)

$$M_{pl} = \frac{E(1 - \xi)}{(1 + \nu)[(1 - 2\nu)(1 - \alpha) + (1 - \alpha\xi)]\xi}, \quad (1)$$

where E and ν are the Young's modulus and Poisson's ratio of the homogeneous solid matrix, respectively, α is a geometrical factor depend on the arrangement of pores and $\alpha=1/3$ for mesoporous materials with a triangular lattice, and $\xi = a^2/c^2$ is a dimensionless porosity factor related to the porosity φ of the porous material by $\xi = \pi/2\sqrt{3} \cdot \varphi$ for a triangular lattice. Note that the porosity discussed in the following is defined after the coating procedure. It can be found that the pore-load modulus depends on the material properties (E and ν), porosity φ , and the geometrical arrangement factor α .

It is noted that most mesoporous materials are functionalized by surface coating. The existing of coating phases affects the overall mechanical properties of the inhomogeneous composite structures. To explore the influence of the pore surface coating on the adsorption-induced deformation of mesoporous materials, the unit cell of coated structure can be treated as bilayer hollow cylinder, in which the inner layer is either uniform or functionally graded coating phase subjected inner pressure p_i , and the outer layer is a homogeneous matrix subjected the outer pressure p_o (see Fig. 1(b) and (c)). The matrix and uniform coating are linear elastic and isotropic, with Young's modulus being E_2 and E_1 , respectively. The graded coating

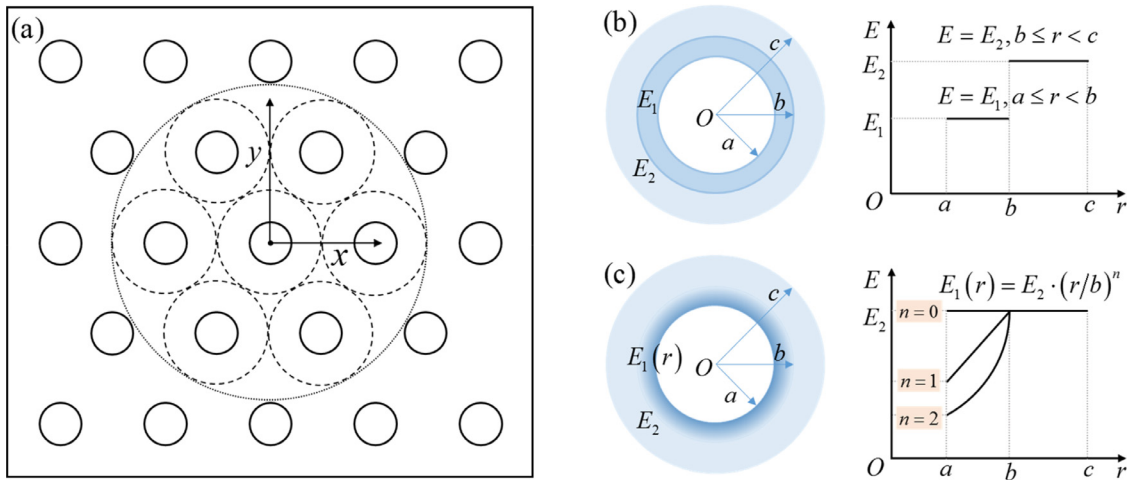


Fig. 1. (a) Two-dimensional schematic of an ordered porous material consisting of parallel cylindrical pores distributed on a triangular lattice. The Young's modulus distribution for the bilayer thick-wall cylinder unit cell with (b) uniform coating and (c) functionally graded coating in the radial direction.

is also assumed to be linear elastic with varying Young's modulus $E_1(r)$ along the radial direction. The Poisson's ratios of the matrix and coating are the same, i.e., ν .

2.1. Mesoporous materials with uniform coating

For mesoporous materials with uniform coating, the elastic solution of the corresponding unit cell (i.e., bilayer cylinder) subjected to inner pressure p_i and outer pressure p_o is given by (Timoshenko & Gere, 2009)

$$\sigma_r^{(i)} = 2C_i + \frac{A_i}{r^2}, \quad \sigma_\theta^{(i)} = 2C_i - \frac{A_i}{r^2}, \quad (2)$$

where $\sigma_r^{(i)}$ and $\sigma_\theta^{(i)}$ are the radial and circumferential stresses, respectively, and $i=1$ and 2 refer to the inner and outer layer, respectively, and the constants A_i and C_i are determined by boundary conditions. The radial displacements are given by

$$u_r^{(i)} = \frac{1+\nu}{E_i} \left[2(1-2\nu)C_i r - \frac{A_i}{r} \right]. \quad (3)$$

By denoting with a and c respectively the inner and the outer radius and with b the radius at the interface between the coating and the homogeneous cylinder (where $t = b - a$ is the thickness of coating layer), the boundary conditions are given as

$$\sigma_r^{(1)} \Big|_{r=a} = -p_i, \quad \sigma_r^{(2)} \Big|_{r=c} = -p_o. \quad (4)$$

As pointed out by Liu et al. (2016) for the case without coating, the inner pressure p_i is the pressure exerted on the pore wall by fluid, and the outer pressure p_o is induced by the interaction between the neighboring pores and can be obtained as

$$p_o = \alpha \left(\frac{a}{c} \right)^2 p_i. \quad (5)$$

Furthermore, the radial displacement and the radial stress are continuous at the interface, that is

$$\sigma_r^{(1)} \Big|_{r=b} = \sigma_r^{(2)} \Big|_{r=b}, \quad u_r^{(1)} \Big|_{r=b} = u_r^{(2)} \Big|_{r=b}. \quad (6)$$

Using Eqs. (2)–(6), the constants A_i and C_i and the stress and displacement fields can be determined.

Accordingly, the pore-load modulus of mesoporous material can be obtained by the definition $M_{pl} = p_i/\varepsilon_e$ with $\varepsilon_e = u_r^{(2)}(c)/c$,

$$M_{pl} = \frac{\lambda_1 E_1 - \lambda_2 E_2}{(1+\nu)[(1-2\nu)m - n]}, \quad (7)$$

where λ_1, λ_2, m and n are constants given below

$$\begin{cases} \lambda_1 = -\left(1 - \frac{b^2}{a^2}\right)\left(\frac{1-2\nu}{1-\nu}\right) - \left(\frac{c^2}{b^2} - \frac{c^2}{a^2}\right)\left(\frac{1}{1-\nu}\right) \\ \lambda_2 = \left(1 - \frac{c^2}{b^2}\right)\left(\frac{1}{1-\nu}\right) + \left(\frac{b^2}{a^2} - \frac{c^2}{a^2}\right)\left(\frac{1-2\nu}{1-\nu}\right) \\ m = \alpha \left\{ \frac{E_1}{E_2} \left(\frac{a^2}{b^2} - 1\right)\left(\frac{1}{1-\nu}\right) - \left[\frac{a^2}{b^2} \left(\frac{1}{1-\nu}\right) + \left(\frac{1-2\nu}{1-\nu}\right) \right] \right\} + 2 \\ n = \alpha \left\{ \frac{E_1}{E_2} \left(\frac{a^2}{c^2} - \frac{b^2}{c^2}\right)\left(\frac{1-2\nu}{1-\nu}\right) + \left[\frac{a^2}{c^2} \left(\frac{1}{1-\nu}\right) + \frac{b^2}{c^2} \left(\frac{1-2\nu}{1-\nu}\right) \right] \right\} - 2 \end{cases} \quad (8)$$

It can be found that the pore-load modulus of coated mesoporous materials depends on not only the elastic modulus and Poisson's ratio of matrix and coating, E_i, ν , but also the geometric dimensions, a, b , and c . It also depends on the geometric arrangement through the factor α . If the porosity factor is defined as $\xi = a^2/b^2$, it can be related to the porosity φ by the relation $\varphi = 2\sqrt{3}/\pi \cdot \xi$ for a triangular lattice. For a porous material under plane stress condition, the parameters E_i and ν need be replaced by $E_i/(1-\nu^2)$ and $\nu/(1-\nu)$, respectively. As a limiting case of no-coating (e.g. $t = 0$), or the coating layer has the same properties as the matrix, Eq. (7) reduces to the classical homogeneous case, i.e., Eq. (1).

2.2. Mesoporous materials with functionally graded coating

For a mesoporous material with functionally graded coating, the corresponding elastic solution of a pressurized hollow cylinder with gradient coating (Fig. 1(c)) was given by Sburлатi (2012) in which the Young's modulus of the coated layer is assumed to be

$$E_1(r) = E_2 \cdot (r/b)^n, \quad (9)$$

where E_2 is the Young's modulus of homogeneous matrix and n is the power index. The displacement component in the radial direction can be expressed as (Sburлатi, 2012)

$$u_r^{(1)} = r^{-n/2} (B_1 r^{-k/2} + B_2 r^{k/2}), \quad (10)$$

where B_1 and B_2 are the constants to be determined by the boundary conditions, and the parameter k is

$$k = -\sqrt{[n^2 + 4 - (2+n)^2\nu]/(1-\nu)}. \quad (11)$$

The corresponding stress components are

$$\begin{cases} \sigma_r^{(1)} = \frac{r^{n/2-1}}{a^n} [r^{-k/2}((n+k)(\nu-1) + 2\nu)\bar{B}_1 + r^{k/2}((n-k)(\nu-1) + 2\nu)\bar{B}_2] \\ \sigma_\theta^{(1)} = -\frac{r^{n/2-1}}{a^n} [r^{-k/2}((n+k)\nu + 2(\nu-1))\bar{B}_1 + r^{k/2}((n-k)\nu + 2(\nu-1))\bar{B}_2] \end{cases} \quad (12)$$

where

$$\bar{B}_i = \frac{E_2}{2(1+\nu)(1-2\nu)} B_i, \quad (\text{for } i = 1, 2). \quad (13)$$

The stress and displacement components of the matrix are the same as shown in the Eqs. (2) and (3) with superscript $i = 2$. Combining the boundary conditions, Eq. (4), and the continuity conditions, Eq. (6), the constants (B_1, B_2, A_2 and C_2) and the stress and displacement fields can be determined.

As the same as the uniform coating case, the pore-load modulus can be obtained by combining the definition $M_{pl} = p_i/\varepsilon_e$ with $\varepsilon_e = u_r^{(2)}(c)/c$ as

$$M_{pl} = \frac{b^2 + c^2 - 2b^2\nu}{\alpha(b^2 - c^2)a^2/E_2c^2 + 2(1-\nu)b^{1-n/2}(gb^{k/2} + hb^{-k/2})}, \quad (14)$$

where g and h are constants given by

$$\begin{cases} g = \frac{2(1-\nu)\alpha\beta_1 a^2 b - a^{1-(n-k)/2} b^{(n-k)/2} [\beta_1(b^2 + c^2 - 2b^2\nu) + 2(1-2\nu)(b^2 - c^2)]}{E_2 b^{-n/2} [\beta_1\beta_2(b^2 + c^2 - 2b^2\nu)(b^{-k/2}a^k - b^{k/2}) + 2(1-2\nu)(b^2 - c^2)(\beta_1 b^{k/2} + \beta_2 b^{-k/2}a^k)]} \\ h = \frac{a^{1-(n-k)/2}}{\beta_1 E_2} + \frac{\beta_2 a^k}{\beta_1} g, \quad \text{where } \beta_1 = (k+n)(1-\nu) - 2\nu, \beta_2 = (k-n)(1-\nu) + 2\nu \end{cases} \quad (15)$$

Similar to the uniform coating case, the pore-load modulus of the functionally graded coated mesoporous material is related to the mechanical properties of homogeneous matrix (E_2 and ν), the porosity φ , the geometric dimensions a, b , and c , and the geometrical arrangement factor α . It also depends on the variation of Young's modulus through the power index n . However, different from the uniform coating case, there is no jump of the properties at the interface between the

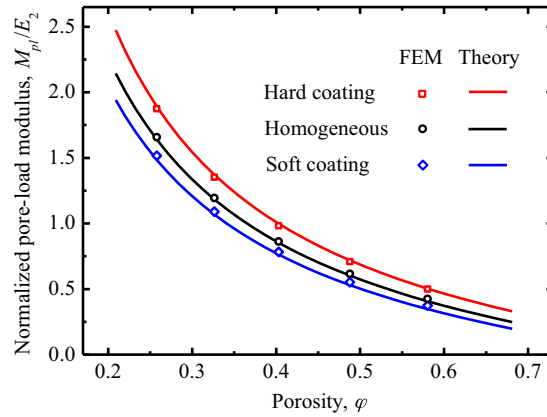


Fig. 2. Comparison of FEM simulations (symbols) and theoretical predictions (lines) of the normalized pore-load moduli as a function of porosity for the mesoporous materials with uniform coating.

coated layer and matrix of the functionally graded coating. For the limiting case of $t = 0$ or $n = 0$, Eq. (15) reduces to the classical model (i.e., Eq. (1)) for the homogeneous mesoporous materials.

Furthermore, it should be noted that there is another limiting case, the functionally graded mesoporous material, can be obtained when the thickness of the homogeneous matrix approaching zero (i.e., $b = c$ in Fig. 1(c)). Thus, Eq. (14) reduces to

$$M_{pl} = \frac{E_2(1 - \xi^{k/2})/[2(1 + \nu)(1 - 2\nu)]}{\left[\xi^{(2-n+k)/4} - \alpha\xi^{(2+k)/2}\right]/\beta_1 + \left[\xi^{(2-n+k)/4} - \alpha\xi\right]/\beta_2}, \quad (16)$$

where β_1 and β_2 are the parameters as above given by Eq. (15). Here, $\xi = a^2/c^2$ is the above-mentioned porosity factor. If the power index n takes 0, i.e., the Young's modulus of the matrix is uniform, we can get the degenerated classical result (see Eq. (1)) for the homogeneous case.

3. FEM simulation and results analysis

In order to validate the obtained analytical results for the pore-load modulus, the adsorption-induced deformation of ordered mesoporous materials with uniform and functionally graded coating is calculated numerically by FEM simulations using the commercially available software package ANSYS 12.0.

3.1. Finite element model

A plate with parallel cylindrical pores distributed on a triangular lattice (see Fig. 1(a)) was considered for FEM simulation. The boundary conditions of the numerical model are defined as: the left and bottom surfaces are constrained in x and y directions, respectively, while the right and top surface could move freely to ensure that the porous plate can freely contract or expand under the applied pressure within the pore space. Numerical experiment shows that a model with the number of 15×17 unit cells for triangular lattice is sufficient to show the homogenized responses of the porous materials. Moreover, mesh sensitivity study has been conducted a priori to ensure the numerical convergence of the FE models.

For the porous material with uniform coating, as shown in Fig. 1(b), the constituent solid matrix is assumed to be linearly elastic with Young's modulus $E_2 = 130$ GPa. Three different cases are taken into account, i.e., soft coating with $E_1 = 80$ GPa, homogeneous case with $E_1 = 130$ GPa, and hard coating with $E_1 = 210$ GPa. Poisson's ratio of both matrix and coating is $\nu = 0.28$. For the porous material with functionally graded coating, as shown in Fig. 1(c), the matrix is also chosen to be $E_2 = 130$ GPa and $\nu = 0.28$. The properties of the coating layer are controlled by the power law with index n . In this study, $n = -2, -1, 0, 1$ and 2 are considered. Based on the convergence analysis, the non-uniform Young's modulus are implemented by separating the graded coating into ten layers with stepwise linear elastic modulus.

3.2. Results and analysis

3.2.1. Uniform coating

First, consider the deformation of a mesoporous material with uniform coating (Fig. 1(b)). The coating thickness is chosen to be $t/c = 1/15$, as an example, in the simulation. The FEM predicted porosity-dependent pore-load moduli of the porous material, normalized by the Young's modulus of the solid matrix, are shown in Fig. 2 as symbols. Three cases (i.e., soft coating, homogeneous, and hard coating) are considered. The corresponding theoretical predictions given by Eq. (7) are

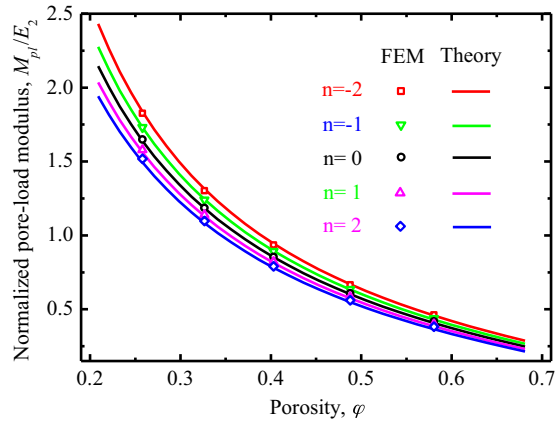


Fig. 3. Comparison of FEM simulations (symbols) and theoretical predictions (lines) of the normalized pore-load moduli as a function of porosity for the mesoporous materials with functionally graded coating.

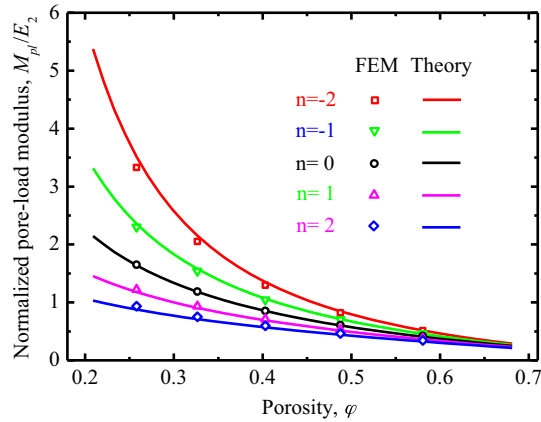


Fig. 4. Comparison of FEM simulations (symbols) and theoretical predictions (lines) of the normalized pore-load moduli as a function of porosity for functionally graded mesoporous materials.

also included as lines for the purpose of comparison. For all three cases, one can find that the theoretical model can accurately predict the FEM results. It also shows that the elastic properties of coating layer have significant effect on the overall deformation of the coated mesoporous material under inner pressure. If the porous material is coated with hard layer, the pore-load modulus is higher than the homogeneous one. Conversely, the soft coating layer induces lower pore-load modulus.

3.2.2. Functionally graded coating

For the mesoporous material with functionally graded coating, as shown in Fig. 1(c), the coating thickness is chosen as $t/c = 2/15$ in the simulation. The normalized pore-load moduli given by the FEM simulations and theoretical predictions (Eq. (14)) are shown in Fig. 3. The results of selected power indexes $n = 0, \pm 1, \pm 2$ are presented by different colors. It shows that the pore-load modulus is a function of the porosity of the mesoporous sample and the theoretical predictions are consistent with the FEM simulations. Similar to the uniform coating cases, the functionally graded coating layer also affects the overall deformation of the coated mesoporous materials. With the hard coating layer, i.e., power index $n < 0$, the pore-load modulus is higher; for the soft coating layer ($n > 0$), the pore-load modulus is lower than the homogeneous case ($n = 0$).

Additionally, as a special case of the solution for functionally graded coatings, the deformation of the functionally graded mesoporous materials are also numerically simulated by FEM and, the normalized pore-load moduli are plotted in Fig. 4 with symbols. The theoretical predictions (Eq. (16)) are included as lines for comparison. Five distributions of the Young's modulus (dependent on the power index n) are considered. It can be found that the theoretical model can predict the FEM simulations well for all the five cases. The distribution of Young's modulus has significant effect on the deformability to the inner pressure, i.e., the value of pore-load moduli dependent on the power index. The relative difference of these cases will decrease with increasing of the porosity of the material. This is due to the fact that the higher porosity means smaller difference of the Young's modulus along the radial direction.

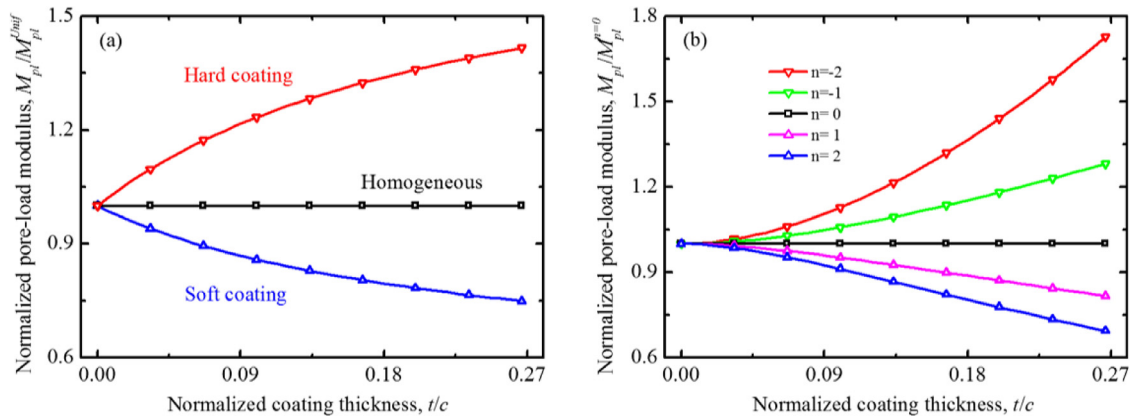


Fig. 5. The normalized pore-load moduli varies as a function of coating thickness for the mesoporous materials with (a) uniform coating and (b) functionally graded coating.

4. Discussions

4.1. The effect of coating thickness

Generally, thickness of the coating layer affects the overall deformation of the coated composite structures. All the cases discussed in the previous sections are focus on the relationship between the pore-load modulus and porosity. Here, we discuss the effects of coating thickness on the pore-load modulus of the coated mesoporous materials. Both uniform coating and functionally graded coating are considered. To simplify the analysis, we fix the porosity at $\varphi = 0.15$ in the following discussions.

The theoretical predictions of the normalized pore-load modulus are plotted as a function of the normalized coating thickness in Fig. 5. It can be found that, for both the uniform coating (Fig. 5(a)) and functionally graded coating (Fig. 5(b)) cases, the hard coating layer induces larger pore-load modulus than the homogenous case, and the soft coating layer induces smaller one. Furthermore, influence of the coating layer on the pore-load modulus becomes more significant with the thickness increasing for both two cases. It can also be found the trends of the pore-load modulus varies with the coating thickness are slowing down for uniform coating cases but getting faster for the functionally graded coating cases. This difference is induced by the different Young's modulus distributions of the coating layers.

4.2. The effect of relative Young's modulus

For the mesoporous materials with uniform or functionally graded coatings, the relative Young's modulus (i.e., the ratio between the modulus of coating layer E_1 and matrix E_2) affects the overall adsorption-induced deformations. In order to investigate their relationships quantitatively, the theoretical predictions of the normalized pore-load moduli are plotted as a function of the relative Young's modulus. As mentioned above, to simplify the analysis, the porosity and the relative coating thickness are fixed as constants (i.e., $\varphi = 0.15$ and $t/c = 2/15$) in the following discussions. Note that the modulus of the functionally graded coating layer is varying with the radial position as a function of $E_1(r)$, we choose the value at the inner boundary $E_1(a)$ as a reference.

It is seen from Fig. 6 that the normalized pore-load moduli increase with increasing of the relative Young's moduli for both the uniform and functionally graded coating cases. As we have defined above, $E_1/E_2 < 1$ (or $E_1(a)/E_2 < 1$) reflects a soft coating, conversely, $E_1/E_2 > 1$ (or $E_1(a)/E_2 > 1$) indicates a hard coating. For the hard coating cases, a larger modulus of the coating layer induces a larger pore-load modulus in both two cases with an accelerating trend. On the contrary, a smaller modulus of the coating layer induces a smaller pore-load modulus for the soft coating cases with a slowing trend. For the uniform coating cases, as shown in Fig. 6(a), when the relative Young's modulus $E_1/E_2 \ll 1$, e.g. the coating layer is much softer than the matrix, the pore-load modulus is approaching a convergence value, which is equal to the modulus calculated from the mesoporous material without the coating layer. The same asymptotic trend in the soft coating regime can also be found in the functionally graded coating cases (see Fig. 6(b)), but it is less conspicuous.

The analytical solutions developed in this paper provide an instructive tool to analysis the coated mesoporous materials. As a typical example, Elam, Routkevitch, Mardilovich, and George (2003) performed an experiment to fabricate coated anodic alumina (AA) membranes to improve their surface properties by depositing Al_2O_3 or ZnO on the pore surface. In their study, the initial pore diameter of the porous AA membranes is about 65 nm. After coating, the pore diameter reduced to 39 nm. The porosity of the as-fabricated AA membranes is chosen as 45.0%, the porosity after coating can be calculated as about 16.2%. Considering the Al_2O_3 coated membranes, the elastically properties of the matrix and coated layer (Daehn et al., 1996) are $E_{\text{Al}} = 70$ GPa, $E_{\text{Al}_2\text{O}_3} = 380$ GPa and $\nu = 0.3$, the pore-load modulus of the coated sample is

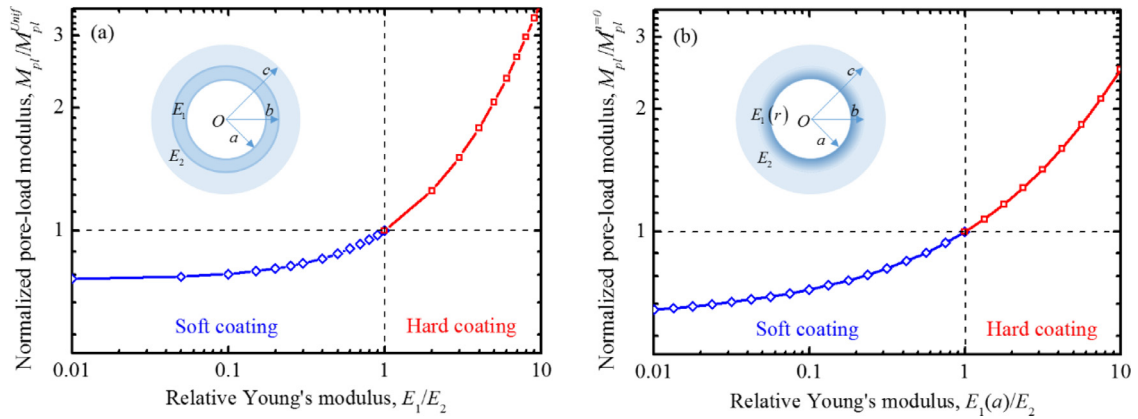


Fig. 6. The normalized pore-load moduli varies as a function of relative Young's moduli for the mesoporous materials with (a) uniform coating and (b) functionally graded coating.

about $M_{pl}^{Al_2O_3} = 930$ GPa calculated from Eq. (7). For the ZnO coated membranes, the Young's modulus of the coated layer (Kucheyev et al., 2002) is $E_{ZnO} = 110$ GPa, the corresponding pore-load modulus of the coated material can be calculated about $M_{pl}^{ZnO} = 295$ GPa. If the different elastic moduli of the coated layer are not considered, the corresponding pore-load modulus can be calculated as $M'_{pl} = 215$ GPa with about 77% and 27% underestimation of the actual pore-load modulus for Al_2O_3 and ZnO coated membranes, respectively. It can be found that the coated layer obviously affects the overall response of the mesoporous material to pore pressure.

5. Concluding remarks

The adsorption-induced deformation of ordered mesoporous materials with coatings are investigated theoretically and numerically by a two-dimensional micromechanical model, which is based on the single pore model of a pressurized bilayer thick-wall cylinder unit cell. For both the uniform coating and functionally graded coating cases, the close-form analytical solutions of the pore-load modulus are derived on the basis of the single pore model. The derived analytical solutions for both the two types of coating cases can reduce to the homogenous case. The proposed theoretical models are validated by comparing with FEM simulations. Excellent agreement between them is achieved with the maximum relative error smaller than 5%.

The model predictions clearly reveal that the coating layer plays an important role on the overall elastic response of coated mesoporous materials to inner pressure for both the uniform coating and functionally graded coatings, and the pore-load modulus shows significant dependence on the coating thickness and the relative Young's modulus for both coating cases. In particular, significant differences in pore-load modulus can be observed for mesoporous materials with low porosity, relative thick coating layer ($t/c > 0.05$) and with distinct elastic properties of the coating material ($E_1/E_2 < 0.8$ or $E_1/E_2 > 1.2$). The present model can be applied to a large class of materials with mesoporous morphologies. Moreover, our findings can be used to design mesoporous material based sensors and actuators in various applications.

Acknowledgments

The authors are grateful for the financial support of this work by the National Natural Science Foundation of China (No. 11472149) and the Tsinghua University Initiative Scientific Research Program (No. 2014z22074).

References

- Amato, G., Delerue, C., & VonBardeleben, H. (1998). *Structural and optical properties of porous silicon nanostructures*. CRC Press.
- Bellet, D., Lamagnere, P., Vincent, A., & Brechet, Y. (1996). Nanoindentation investigation of the Young's modulus of porous silicon. *Journal of Applied Physics*, 80, 3772–3776.
- Biener, J., Wittstock, A., Zepeda-Ruiz, L., Biener, M., Zielasek, V., Kramer, D., et al. (2009). Surface-chemistry-driven actuation in nanoporous gold. *Nature Materials*, 8, 47–51.
- Birman, V. (2014). Mechanics and energy absorption of a functionally graded cylinder subjected to axial loading. *International Journal of Engineering Science*, 78, 18–26.
- Bonfoh, N., Coulibaly, M., & Sabar, H. (2014). Effective properties of elastic composite materials with multi-coated reinforcements: A new micromechanical modelling and applications. *Composite Structures*, 115, 111–119.
- Canham, L. (2014). *Handbook of porous silicon*. Springer.
- Chen, Y. J., Li, Y., Chu, B., Kuo, I. T., Yip, M., & Tai, N. (2015). Porous composites coated with hybrid nano carbon materials perform excellent electromagnetic interference shielding. *Composites Part B: Engineering*, 70, 231–237.
- Cherkaoui, M., Sabar, H., & Berveiller, M. (1995). Elastic composites with coated reinforcements: A micromechanical approach for nonhomothetic topology. *International Journal of Engineering Science*, 33, 829–843.

- Daehn, G., Starck, B., Xu, L., Elifshawy, K., Ringnalda, J., & Fraser, H. (1996). Elastic and plastic behavior of a co-continuous alumina/aluminum composite. *Acta Materialia*, 44, 249–261.
- David, E., & Zimmerman, R. W. (2011). Elastic moduli of solids containing spheroidal pores. *International Journal of Engineering Science*, 49, 544–560.
- Davis, M. E. (2002). Ordered porous materials for emerging applications. *Nature*, 417, 813–821.
- Dolino, G., Bellet, D., & Faivre, C. (1996). Adsorption strains in porous silicon. *Physical Review B*, 54, 17919.
- Dourdain, S., Britton, D., Reichert, H., & Gibaud, A. (2008). Determination of the elastic modulus of mesoporous silica thin films by x-ray reflectivity via the capillary condensation of water. *Applied Physics Letters*, 93, 183108.
- Duan, H., Wang, J., Karihaloo, B., & Huang, Z. (2006). Nanoporous materials can be made stiffer than non-porous counterparts by surface modification. *Acta Materialia*, 54, 2983–2990.
- El Kadib, A., Finiels, A., & Brunel, D. (2013). Sulfonic acid functionalised ordered mesoporous materials as catalysts for fine chemical synthesis. *Chemical Communications*, 49, 9073–9076.
- Elam, J., Routkevitch, D., Mardilovich, P., & George, S. (2003). Conformal coating on ultrahigh-aspect-ratio nanopores of anodic alumina by atomic layer deposition. *Chemistry of Materials*, 15, 3507–3517.
- Fateh, R., Ismail, A. A., Dillert, R., & Bahnemann, D. W. (2011). Highly active crystalline mesoporous TiO₂ films coated onto polycarbonate substrates for self-cleaning applications. *The Journal of Physical Chemistry C*, 115, 10405–10411.
- Faustini, M., Nicole, L., Boissiere, C., Innocenzi, P., Sanchez, C., & Grosso, D. (2010). Hydrophobic, antireflective, self-cleaning, and antifogging sol-gel coatings: An example of multifunctional nanostructured materials for photovoltaic cells. *Chemistry of Materials*, 22, 4406–4413.
- Feng, X., Fryxell, G., Wang, L.-Q., Kim, A. Y., Liu, J., & Kemner, K. (1997). Functionalized monolayers on ordered mesoporous supports. *Science*, 276, 923–926.
- Findenegg, G. H., Jähnert, S., Mütter, D., Prass, J., & Paris, O. (2010). Fluid adsorption in ordered mesoporous solids determined by in situ small-angle X-ray scattering. *Physical Chemistry Chemical Physics*, 12, 7211–7220.
- Günther, G., Prass, J., Paris, O., & Schoen, M. (2008). Novel insights into nanopore deformation caused by capillary condensation. *Physical Review Letters*, 101, 086104.
- Gor, G. Y., & Neimark, A. V. (2010). Adsorption-induced deformation of mesoporous solids. *Langmuir*, 26, 13021–13027.
- Gor, G. Y., & Neimark, A. V. (2011). Adsorption-induced deformation of mesoporous solids: Macroscopic approach and density functional theory. *Langmuir*, 27, 6926–6931.
- Gor, G. Y., Bertineti, L., Bernstein, N., Hofmann, T., Fratzl, P., & Huber, P. (2015). Elastic response of mesoporous silicon to capillary pressures in the pores. *Applied Physics Letters*, 106, 261901.
- Grosman, A., Puibasset, J., & Rolley, E. (2015). Adsorption-induced strain of a nanoscale silicon honeycomb. *EPL (Europhysics Letters)*, 109, 56002.
- Herman, T., Day, J., & Beamish, J. (2006). Deformation of silica aerogel during fluid adsorption. *Physical Review B*, 73, 094127.
- Horikawa, T., Do, D., & Nicholson, D. (2011). Capillary condensation of adsorbates in porous materials. *Advances in Colloid and Interface Science*, 169, 40–58.
- Innocenzi, P., & Malfatti, L. (2013). Mesoporous thin films: Properties and applications. *Chemical Society Reviews*, 42, 4198–4216.
- Kucheyev, S., Bradby, J., Williams, J., Jagadish, C., & Swain, M. (2002). Mechanical deformation of single-crystal ZnO. *Applied Physics Letters*, 80, 956–958.
- Liu, M., Wu, J., Gan, Y., & Chen, C. Q. (2016). The pore-load modulus of ordered nanoporous materials with surface effects. *AIP Advances*, 6, 035324.
- McInnes, S. J. P., Szili, E., Al-Bataineh, S. A., Vasani, R. B., Xu, J., Alf, M. E., et al. (2015). Fabrication and characterization of a porous silicon drug delivery system with an iCVD temperature-responsive coating. *Langmuir*, 32, 301–308.
- Melde, B. J., Johnson, B. J., & Charles, P. T. (2008). Mesoporous silicate materials in sensing. *Sensors*, 8, 5202–5228.
- Mohammadi, M., Saha, G., & Akbarzadeh, A. (2016). Elastic field in composite cylinders made of functionally graded coatings. *International Journal of Engineering Science*, 101, 156–170.
- Muroyama, N., Yoshimura, A., Kubota, Y., Miyasaka, K., Ohsuna, T., Ryoo, R., et al. (2008). Argon adsorption on MCM-41 mesoporous crystal studied by in situ synchrotron powder X-ray diffraction. *The Journal of Physical Chemistry C*, 112, 10803–10813.
- Niu, B., & Yan, J. (2015). A new micromechanical approach of micropolar continuum modeling for 2-D periodic cellular material. *Acta Mechanica Sinica*, 32, 456–468.
- Prass, J., Mütter, D., Fratzl, P., & Paris, O. (2009). Capillarity-driven deformation of ordered nanoporous silica. *Applied Physics Letters*, 95, 083121.
- Rasaiah, J. C., Garde, S., & Hummer, G. (2008). Water in nonpolar confinement: From nanotubes to proteins and beyond. *Annu. Rev. Phys. Chem.*, 59, 713–740.
- Sailor, M. J. (2012). *Porous silicon in practice: Preparation, characterization and applications*. John Wiley & Sons.
- Sburlati, R. (2012). Analytical elastic solutions for pressurized hollow cylinders with internal functionally graded coatings. *Composite Structures*, 94, 3592–3600.
- Timoshenko, S. P., & Gere, J. M. (2009). *Theory of elastic stability*. Courier Corporation.
- Van Rhijn, W., De Vos, D., Sels, B., & Bossaert, W. (1998). Sulfonic acid functionalised ordered mesoporous materials as catalysts for condensation and esterification reactions. *Chemical Communications*, 317–318.
- Wang, G., & Pindera, M.-J. (2016). Locally-exact homogenization of unidirectional composites with coated or hollow reinforcement. *Materials & Design*, 93, 514–528.